PROCEEDINGS OF SCIENCE

Investigation of In-Medium Hadron Properties by Azimuthal Emission Patterns of K^+ and K^-

Tae Im Kang* **(for the FOPI Collaboration)**
Heidelberg University
E-mail: kang@physi.uni-heidelberg.de

Modification of hadron properties in hot and dense nuclear matter is a topic of great interest. Kaons, which are produced in nucleus-nucleus collisions at sub-threshold energies at SIS in GSI, are very promising particles to investigate in-medium effects on hadrons. Azimuthal emission patterns of K^+ and K^- mesons have been measured in Ni+Ni collisions with the FOPI spectrometer at beam kinetic energy of 1.91A GeV to investigate an in-medium potential in dense baryonic matter. The presented results show the different propagation patterns of K^+ and K^- mesons inside the dense nuclear medium and indicate the existence of a kaon-nucleon potential, repulsive for K^+ and attractive for K^- comparing to the predictions of theoretical model.

Sixth International Conference on Quarks and Nuclear Physics
April 16-20, 2012
Ecole Polytechnique, Palaiseau, Paris

*Speaker.

PoS(QNP2012)174

1. Introduction

Relativistic heavy-ion collisions at incident energies range of 1-2A GeV provide a unique opportunity to study both the properties of hadrons in dense nuclear matter and the behavior of nuclear matter at high densities [1]. The possible modification of hadron masses and widths in hot and dense matter is a subject of great current interest. In particular the investigations of the in-medium properties of kaons is important for understanding chiral symmetry restoration [2].

1.1 Kaons in dense nuclear matter

As a consequence of chiral symmetry restoration in hot and dense nuclear matter, the effective mass of charged kaons are expected to be modified with increasing baryon density. Various model calculations agree qualitatively on their predictions of the total energy of K mesons at rest in nuclear matter as function of density [3]. According to the calculations, the effective mass of K^+ mesons increases moderately with increasing baryon density whereas the effective mass of K^- mesons decreases significantly. Mean-field calculations predict this effect is caused by a repulsive K^+-nucleon potential and an attractive K^--nucleon potential. This in-medium K-nucleon potential in dense hadronic matter is expected to manifest itself in their azimuthal emission pattern with respect to the reaction plane [4].

1.2 Azimuthal emission patterns

The phenomenon of collective flow [5] can generally be characterized in terms of anisotropies of the azimuthal emission pattern, expressed by a Fourier series:

$$\frac{dN}{d\phi} \propto (1 + 2v_1 cos(\phi) + 2v_2 cos(2\phi) + ...)\,, \tag{1.1}$$

where ϕ is the azimuthal angle of the outgoing particle with respect to the reaction plane [6]. The first order Fourier coefficient, $v_1 = \langle cos(\phi)\rangle = \langle p_x/p_T\rangle$, describes the sideward deflection of particles in the reaction plane. The second order coefficient, $v_2 = \langle cos(2\phi)\rangle = \langle (p_x/p_T)^2 - (p_y/p_T)^2\rangle$, describes the in-plane/out-of-plane emission pattern with respect to the reaction plane.

2. FOPI ToF upgrade

The FOPI detector [7] is an azimuthally symmetric apparatus comprising several sub detectors (Fig 1, left panel) which provide charge and mass determination over nearly the full solid angle. The identification of charged particles is achieved by the curvature of particle tracks in the magnetic field, by their specific energy loss in the drift chamber, and by the time-of-flight (ToF). Recently FOPI has successfully upgraded the Time-of-Flight detector system with a barrel of Multi-strip Multi-gap Resistive Plate Counters (MMRPC) [8] to improve the charged kaon measurement, Fig. 2. The charged kaons are identified from two ToF systems, MMRPC ($30^\circ < \theta_{lab} < 55^\circ$) and Plastic Scintillator Barrel (Plastic, $55^\circ < \theta_{lab} < 110^\circ$), matched with Central Drift Chamber (CDC, $28^\circ < \theta_{lab} < 135^\circ$).

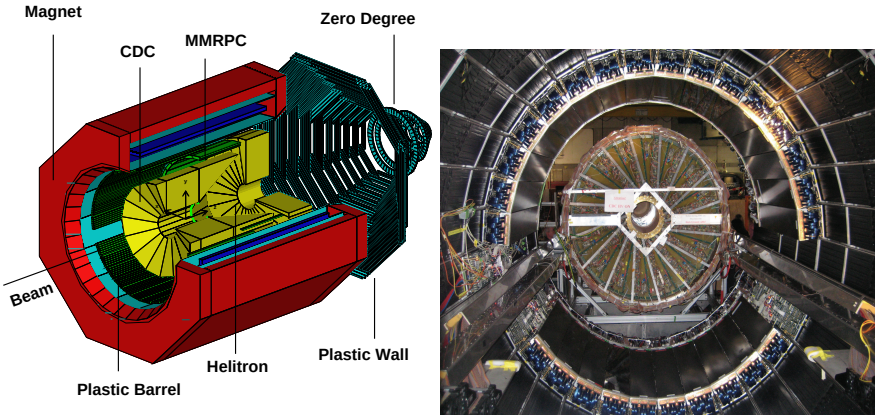

Figure 1: Left panel: setup of the FOPI detector. The target is placed inside of the central drift chamber (CDC), indicated by xyz coordinate arrows. The FOPI detector has cylindrical symmetry around the beam axis. The two drift chambers (CDC and Helitron) and a barrel of scintillator strips and MMRPCs are placed inside the superconducting solenoid magnet. Right panel: photo of MMRPC installed in the FOPI superconducting magnet; CDC is moved out of the magnet.

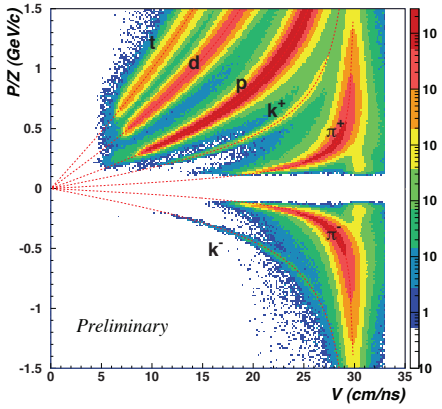

Figure 2: Momentum and velocity correlation using CDC and MMRPC for Z = ±1 particles. Pions, kaons, protons, deuterons and tritons are indicated. With improved system time resolution $\sigma_{ToF} \leq 88$ ps, the charged kaons acceptance was increased to higher momenta, $p < 1$ GeV/c for K^+ mesons and $p < 0.9$ GeV/c for K^- mesons.

3. Results

The FOPI experiment recorded 69×10^6 Ni+Ni collisions, corresponding to the most central 60% of the reaction cross section ($b_{geo} < 7$ fm using the sharp cutoff approximation). The events were centrality selected by imposing conditions on the baryon multiplicity (Mul); defining a central ($48 \leq$ Mul < 90) and a peripheral event ($0 <$ Mul ≤ 47) classes. The corresponding geometrical impact parameter (b_{geo}) ranges are classified using a sharp cut-off approximation; $0 < b_{geo} < 3$ fm and $3 < b_{geo} < 7$ fm for a central and a peripheral event classes, respectively.

3.1 Particle identification of K^+ and K^-

In total, 233,300 K^+ mesons with a signal-to-background-ratio (S/B) better than 10 and 5,200 K^- mesons with S/B better than 4 were identified in the interval of $\pm 2\sigma$ around the nominal kaon

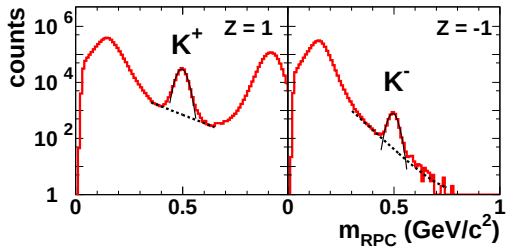

Figure 3: The mass spectra from MMRPC for Z = ±1. The solid and dashed line represent Gaussian fit functions for the kaons and exponential functions for the background, respectively.

mass from the Plastic and MMRPC mass spectra (Fig. 3).

3.2 The FOPI data of v_1 for K^+

In Fig. 4, earlier publications on v_1 of K^+ mesons (circle symbols) and protons (triangle symbols) are presented. The opposite sign of v_1 for K^+ mesons and protons at low p_T demonstrate the existence of a repulsive potential in the dense nuclear medium.

The new experimental data, that presented here, on v_1 of K^+ are also shown in Fig. 4 as square symbols and compared to the old FOPI data (circle symbols) [9] with the same selection of collision centrality ($b_{geo} < 2.55$ fm) and rapidity range ($-1.2 < y_0 < -0.65$, $y_0 = y_{lab}/y_{cm} - 1$). The new data are agreeing with the old FOPI data that were well described by the Relativistic Boltzmann-Uehling-Uhlenbeck (RBUU) model with a repulsive in-medium K^+-nucleon potential of U = 20 MeV.

3.3 Centrality dependence of v_1 for K^+

To study the centrality dependence of v_1 for K^+, two impact parameter ranges, $3 < b_{geo} < 7$ fm (peripheral events) and $b_{geo} < 3$ fm (central events) near target rapidity ($-1.3 < y_0 < -0.5$) are evaluated in Fig. 5. Here there is a clear trend for positive v_1 at low p_T and negative v_1 at high p_T. A change in the v_1 of K^+ pattern can be observed, from central to peripheral collisions. The systematic errors (boxes in Fig. 5) are estimated as 0.024 and 0.012 for peripheral and central collisions, respectively.

In order to evaluate the implications of the data in terms of the properties of $K^\pm$ in the dense nuclear medium, the data are compared to the predictions of Hadron String Dynamics (HSD) model [10] without and with an in-medium potential. The strength of the in-medium K^+-nucleon potential at normal nuclear density and zero momentum was implemented as U = 20 MeV because earlier publications on v_1 of K^+ [9] and the K^0_s spectra [11] could successfully be described by HSD with an in-medium potential of U = 20 ± 5 MeV. Note that only sharp cutoff approximation method was used for the comparison between HSD and the data. However, the model calculations overestimate the magnitude of v_1 for K^+ at low p_T, especially for peripheral collisions in Fig. 5.

3.4 v_1 and v_2 of K^+ and K^-

The experimental data on p_T-integrated v_1 and v_2 for the full event sample ($b_{geo} < 7$ fm) are presented as function of y_0 in Fig. 6. The upper left panel shows positive v_1 for K^+ whereas the values of v_1 for K^- are compatible with zero within the sensitivity of the data as shown in the upper right panel. For a symmetric system, v_1 at mid-rapidity should be zero because v_1 should be antisymmetric with respect to mid-rapidity. This systematic errors (boxes in the upper left panel

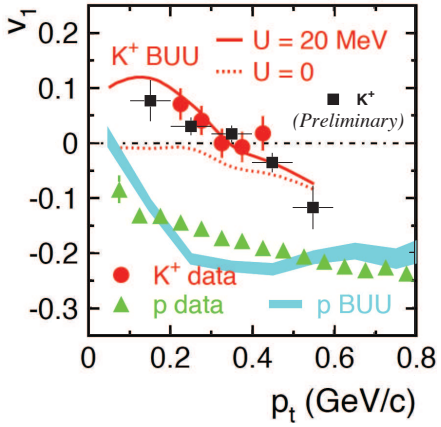

Figure 4: The FOPI data of v_1 for K^+ mesons (circle symbols) and protons (triangle symbols) in the rapidity range $-1.2 < y_0 < -0.65$ for central ($b_{geo} <$ 2.55 fm) Ni+Ni collisions at 1.93A GeV [9]. The preliminary data on v_1 of K^+ (square symbols) are added in the picture which was taken from [9].

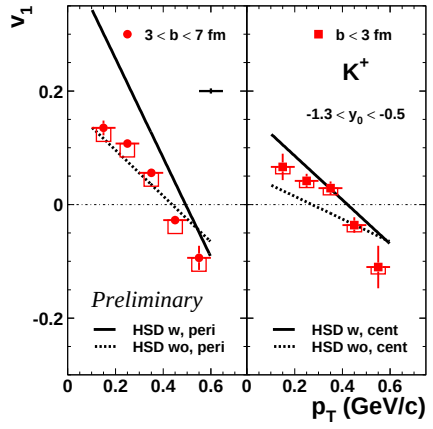

Figure 5: v_1 of K^+ mesons (points) in peripheral (peri) and central (cent) collisions. The data are compared to the HSD calculations with ('w') and without ('wo') in-medium potential. The statistical uncertainty on the HSD calculations shown separately in the upper right side in the left panel.

of Fig. 6) are estimated as 0.020 from the mid-rapidity offset. The lower plots in Fig. 6 show that the v_2 values of K^+ are negative (preferential out-of-plane emission [6]), while those of K^- are compatible with zero within the sensitivity of the data.

The data are compared to the HSD calculations with and without in-medium potential in Fig. 6. As mentioned above, the strength of an in-medium K^+-nucleon potential was implemented as U(K^+) = 20 MeV at normal nuclear matter density with a linear density dependence. A linear K^--nucleon potential of U(K^-) = -50 MeV [12] was employed in the HSD model calculations based on theoretical expectations. With this choice of potential the model predicts that the v_1 values are close to zero without any in-medium potential. But when the finite repulsive in-medium potential is introduced, K^+ mesons are pushed away from protons and therefore v_1 values of K^+ are positive. The model calculations of v_2 for K^+ agree with the data reasonably well, but do not show a strong sensitivity for the in-medium potential.

For negative charged kaons, the model calculations predict that K^- mesons are strongly absorbed by nucleons and thus show v_1 values of K^- are positive without in-medium potential. However, the attractive in-medium potential pulls K^- mesons towards nucleons and therefore v_1 turns from positive to negative. However, the depth of an in-medium potential in the model calculations need to be lowered compared to data. The model calculations of v_2 for K^- show that the introduction of an attractive in-medium potential changes the sign of v_2 from negative (preferential

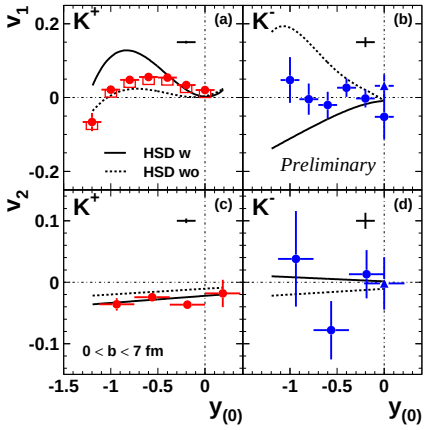

Figure 6: p_T-integrated v_1 of K^+ (a) and K^- mesons (b) and v_2 of K^+ (c) and K^- mesons (d) (points) in comparison to the HSD calculations with ('w') and without ('wo') in-medium potential (see text for details). Error bars on data points denote statistical uncertainties. The statistical uncertainty on the HSD calculations shown separately in the upper right side in each panel.

out-of-plane emission) to positive (preferential in-plane emission), but this effect cannot be verified with the presented data due to large statistical uncertainties.

4. Summary and outlook

In summary, we report on the measurement of the azimuthal emission patterns of K^+ and K^- mesons in Ni+Ni collisions at 1.91A GeV. The data show the different propagation patterns of K^+ and K^- mesons inside the hot and dense nuclear medium and indicate the existence of a kaon-nucleon potential compared to the HSD calculations. However, the origin of the discrepancy between the model calculations and data, especially for the peripheral collisions, has to be investigated in collaboration with theory groups. The measurement of azimuthal patterns of the K^+ and K^- provides valuable information on an in-medium potential in the dense nuclear medium.

References

[1] C. Fuchs, Pro. Part. Nuclear Phys. **56**, 1 (2006).

[2] W. Weise, Prog. Theo. Suppl. 149 (2003) 1.

[3] J. Schaffner-Bielich *et al.*, Nucl. Phys. **A 625**, 325 (1997); M. Lutz, Phys. Lett. B **426**, 12 (1998).

[4] G.Q. Li *et al.*, Phys. Rev. Lett. **74**, 2 (1995).

[5] N. Hermann *et al.*, Annu. Rev. Nucl. Part. Sci. **49**, 581 (1999); Prog. Part. Nucl. Phys. **42**, 187 (1999); W. Reisdorf and H.G. Ritter *et al.*, Ann. Rev. Nucl. Part. Sci. **47**, 663 (1997).

[6] S. Voloshin and Y. Zhang, Z. Phys. C **70**, 665 (1996).

[7] J. Ritman *et al.*, Nucl. Phys. B, Proc., Suppl. **44**, 708 (1995).

[8] M. Kiš *et al.*, Nucl. Instr. and Meth. A **646**, 27 (2011); A. Schüttauf *et al.*, Nucl. Instr. and Meth. A **602**, 679 (2009); Nucl. Phys. B Pro. Supp. **158**, 52 (2006).

[9] P. Crochet *et al.*, Phys. Lett. B **486**, 6 (2000).

[10] W. Cassing *et al.*, Phys. Rep. **308**, 65 (1999).

[11] M.L. Benabderrahmane *et al.*, Phys. Rev. Lett. **102**, 182501 (2009).

[12] W. Cassing *et al.*, Nucl. Phys. A **727**, 59 (2003).